

1 Article

2 Calculation of Reasonable Tension Value for 3 Longitudinal Connecting Reinforcement of CRTSII 4 Slab Ballastless Track

5 Long Chen ¹, Jin-jie Chen ² and Jian-xi Wang ^{2,*}

6 ¹ School of Traffic and Transportation, Shijiazhuang Tiedao University, Shijiazhuang050043, China;
7 chen0244@163.com(L.C.); cjjwxq@126.com(J.-J.C.);

8 ² School of Civil Engineering, Shijiazhuang Tiedao University, Shijiazhuang050043, China;
9 qianxi-2008@163.com(J.-X.W.);

10 * Correspondence: qianxi-2008@163.com; Tel.: +86-15930170825

11

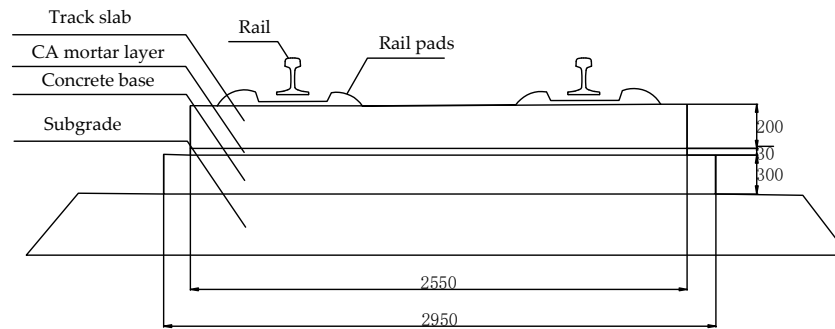
12 **Abstract:** There is a confusion in the original design concept for the tensioning of longitudinally
13 connected reinforcement of CRTSII slab ballastless track. In order to clarify the effect of tension
14 value of longitudinal reinforcement on mechanical characteristics of ballastless track, a three
15 dimensional finite element model considering the nonlinear interaction between the track slab and
16 CA mortar of CRTSII slab ballastless track was established. The mechanical characteristics of the
17 track structure under longitudinal tension load and temperature gradient load of the longitudinal
18 joint were calculated. A method of applying pre-stress to post-pouring concrete was proposed
19 according to the concept of pre-stress loss of pretensioning pre-stressed concrete, reasonable tensile
20 force value was proposed after the crack width and the reinforcement stress of the ballastless track
21 in the operation stage were checked and calculated according to the concrete design principle.
22 When the tension force is greater than 300 kN, it's harmful to the bonding between the slab and
23 mortar layer, which is prone to interlayer damage. In order to adding pre-stress to concrete of wide
24 joints to ensure the longitudinal stability of ballastless track and the reinforcement stress and crack
25 width to meet the design requirements. It is suggested that the tension force value should be 230
26 kN, and the temperature difference between reinforcement and concrete should be 30 °C before the
27 initial curdle of wide joint concrete.

28 **Keywords:** Tension force; Interface damage; CRTSII slab ballastless track; Concrete crack;
29 pre-stress
30

31 1. Introduction

32 Ballastless track which is suitable to the high speed railway for the reason that it has high
33 smoothness and stability of the railway line and has the advantages of high structural stability, good
34 stiffness uniformity, long service life and small maintenance work compared with conventional
35 ballast-track [1,2]. Figure 1 shows the CRTSII slab track and its components. The primary
36 components of the slab track system are the rails, rail pads, track slab, cement emulsified asphalt
37 (CA) mortar layer, and concrete base. CRTSII slab ballastless track is connected longitudinally
38 between track slabs by tensioning the longitudinal connecting reinforcement between track slabs
39 and casting wide and narrow joint concrete [3]. The tensioning of longitudinal reinforcement plays a
40 role in ensuring the longitudinal connection reliable of ballastless track and limiting the crack width
41 at wide and narrow joints. According to the original design concept [4], the tensioning of
42 longitudinal reinforcement generates 300kN prepressure which can effectively reduce the crack
43 width and the stress of the connecting reinforcement on the wide and narrow joint concrete. The

44 wide and narrow joint is an important link in the longitudinal system of CRTSII slab ballastless
 45 track.



46

47

Figure 1. CRTSII slab ballastless track

48 Although the slab track has gained successful improvements and applications in high-speed
 49 railway lines compared with traditional ballasted tracks, slab track still represent some structural
 50 damage caused by train load and temperature load in the operation process. In practice, it is found
 51 that the wide and narrow joint between the track slabs has appeared diseases like concrete falling off
 52 and damage, cracking at joints (shown in Figure 2) and arch etc. in recent years. The longitudinal
 53 continuity and stability of ballastless track are seriously weakened by the damage of the wide and
 54 narrow joint position. Therefore, it is necessary to study the mechanism of wide and narrow joint
 55 disease and provide solutions for the maintenance and repair of wide and narrow joint.



56

57

Figure 2. Cracking at wide and narrow joints

58 At present, most of the researches on wide and narrow joints of ballastless track mainly focus on
 59 the generation of cracks and static and dynamic characteristics of wide and narrow joints under
 60 temperature load and train load. However, it cannot be effectively combined with the construction
 61 process. The influence of wide and narrow joints damage on the force and deformation of seamless
 62 line in temperature rise and continuous high temperature load based on the finite element theory is
 63 studied in reference [5]. The author thinks that there are some problems in the original design
 64 concept that longitudinal connecting reinforcement do not provide pre-pressure on wide joints
 65 concrete. Reference [6] investigated the influence of temperature load, interlayer state and material
 66 quality on the damage of concrete at wide joints using the plastic damage constitutive model of
 67 concrete and analyzed the causes of wide joints damage. Finite element simulation analysis on the
 68 effect of different tension-drawing processes on the force exerted on the rail structure is carried out
 69 in reference [7]. It was concluded that the tension-drawing of the longitudinal reinforcement do not
 70 exert great pre-pressure on the narrow joint concrete, and its effect on temperature resistance is not
 71 obvious. It can be seen that there is a problem of wrong design concept in the longitudinal

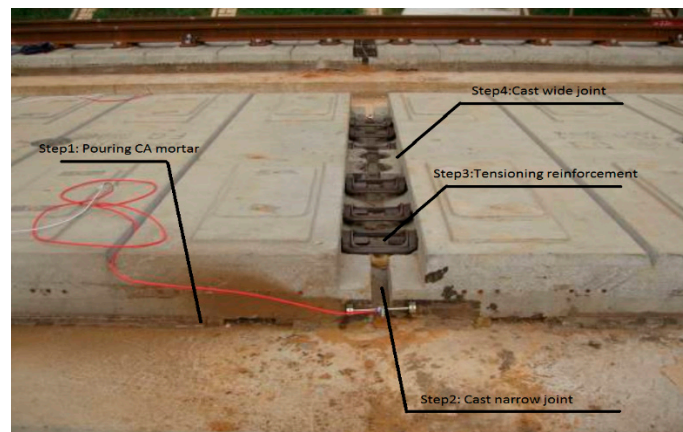
72 connection of ballastless track. However, so far very few studies have been published on the damage
 73 caused by tensioning of longitudinal reinforcement in the construction stage, also there is no
 74 research on fixing this wrong design concept.

75 Based on the above analysis, this paper is divided into two parts (construction stage and
 76 operation stage) to study the tensile properties of longitudinal reinforcement. Firstly, the
 77 construction sequence of CRTSII slab ballastless track in wide and narrow joint position and the
 78 tensioning sequence of longitudinal reinforcement are briefly introduced in section 1. In section 2,
 79 the simulation model in the construction stage is introduced. The interface model parameters are
 80 determined through experimental data. The comparison between numerical results and
 81 experimental measurements is also reported. In section 3, different tension forces are selected as
 82 initial conditions to analyze the stress and deformation of the track structure after tensioning. Also,
 83 the influence of temperature gradient load on the failure of track structure after tensioning is
 84 analyzed according to the environmental changes before the casting of wide joint. In section 4, a
 85 method of applying pre-stress to wide joint concrete is put forward to fixing the error of original
 86 design concept. Reasonable tension force is proposed after the stress of reinforcement and crack
 87 width of concrete at the joint are checked and calculated according to the concrete design principle
 88 [8].

89 2. Longitudinal joint construction of CRTSII slab ballastless track

90 2.1 Construction sequence of ballastless track

91 The construction sequence of ballastless track is shown in the Figure 3 after casting the concrete
 92 base.



93
 94 **Figure 3.** Construction sequence of ballastless track

95 Step1: Pouring CA mortar

96 Check the status of the track slab to make sure that its position meets the design requirements
 97 and prewet the concrete base before the CA mortar is poured. CA mortar is perfused through the
 98 perfusion holes in the middle of the track slab. The CA mortar for each track slab shall be perfused
 99 once for all.

100 Step2: Cast narrow joint concrete

101 The pouring of narrow joint should be carried out after CA mortar perfusion is completed and
 102 its strength reaches 7MPa. The narrow joint height is controlled at the 6 cm below the up edge of the
 103 track slab.

104 Step3: Tensioning longitudinal reinforcement

105 The tensioning process of reinforcement should be carried out after the strength of CA mortar
 106 reaches 9MPa and the strength of narrow joint concrete reaches 20MPa, the specific tensioning
 107 sequence is detailed in section 1.2.

108 Step4: Cast wide joint concrete

109 The concrete should be poured in time after the longitudinal reinforcement is connected.
 110 Re-check the tension force value before casting. After the casting is completed, it should be vibrated
 111 and compacted and make the concrete surface flush with the surface of the track slab.

112 2.2 Tensioning sequence of longitudinal reinforcement

113 Each wide and narrow joint is provided with 6 tension locks, First, tension the middle of the
 114 two locks (inside locks), and then tension two locks near the middle locks(middle locks), at last, the
 115 two locks on the outermost side (outside locks) are tensioned. A total tension force of 300kN is
 116 applied to 6 longitudinal reinforcement for each longitudinal reinforcement tension force is 50kN.

117 Tensioning sequence:

118 Step1:

119 Tension the inside locks of two joints.

120 Step2:

121 Symmetrically tensioning the two inside locks near the two joints that have been stretched.

122 Tensioning step is carried out with two joints step by step.

123 Step3:

124 The middle locks of the two middle joints was tensioned after six inside locks were stretched.

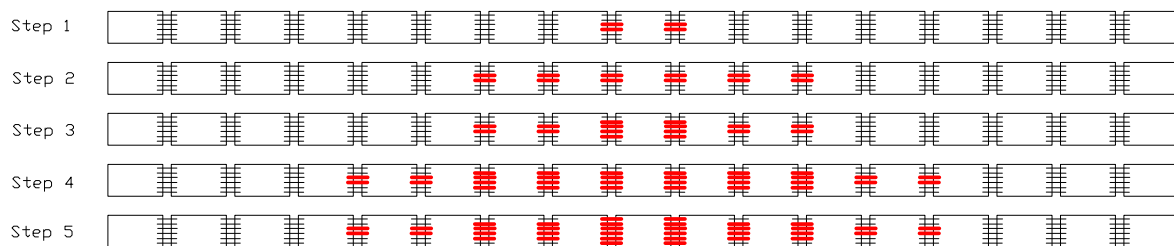
125 Step4:

126 Continue symmetrically tensioning the two inside locks near the joints that have been stretched
 127 and at the same time tensioning the two middle locks near the joints that have been stretched.

128 Step5:

129 The outside locks of the two middle joints was tensioned after six middle locks were stretched.

130 Longitudinal reinforcement is tensioned in this order until the completion of a construction
 131 section. The tensioning sequence is shown in the Figure 4.



132
133 **Figure 4.** Tensioning sequence of longitudinal reinforcement

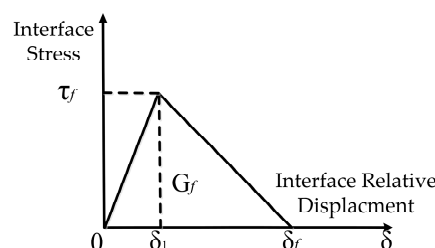
134 3. Calculation model and experimental verification

135 3.1 Cohesive zone model

136 Cohesive zone model (CZM) was introduced by Dugdale and Barrenblatt in 1960 and 1962
 137 respectively [9-11]. CZM has been used for the fracture process analysis of most materials since the
 138 CZM overcomes the inconsistency of the crack tip stress in classical fracture mechanics and can
 139 simply characterize the initiation and propagation of cracks [12-18].

140 In this paper, the CZM is used to simulate the bonding characteristics between the track slab
 141 and the mortar layer. It is assumed that the relationship between the stress of each tiny region of the
 142 cohesive zone and the open displacement (τ - δ) is defined as the bilinear relationship as shown in
 143 Figure 5. This model is suitable for numerical simulation of finite element method.

144



145
146 **Figure 5.** Models of binding-slippage

147 The model is divided into 3 stages. Stage1: Elastic stage. The ultimate bonding strength of the
 148 interface is τ_f , and the corresponding displacement is δ_1 . The interface stress increases linearly before
 149 it reaches the ultimate bonding strength τ_f . Stage2: Softening stage. The interface stress decreases
 150 linearly when the relative displacement is greater than δ_1 . The relative displacement reaches δ_f when
 151 the bonding strength drops to zero. Stage3: Failure stage. The model starts to fail when the relative
 152 displacement is greater than δ_f . G_f is defined as the fracture energy which its value is the area
 153 enclosed by the triangle.

154 The maximum stress criterion is used to describe the initial damage of the interface element.
 155 The damage begins when any nominal stress ratio reaches 1.

$$\max \left\{ \frac{\langle \tau_n \rangle}{\tau_n^0}, \frac{\tau_s}{\tau_s^0}, \frac{\tau_t}{\tau_t^0} \right\} = 1 \quad (1)$$

156
 157 Where τ_n^0 , τ_s^0 , τ_t^0 respectively represent the bonding strength of the normal stress, the first
 158 shear stress, and the second shear stress. τ_n , τ_s , τ_t respectively represents the normal stress and two
 159 shear stresses in the mixed stress mode. Where the brackets $\langle \rangle$ means that the compressive stress
 160 does not contribute to the initial failure of the structure.

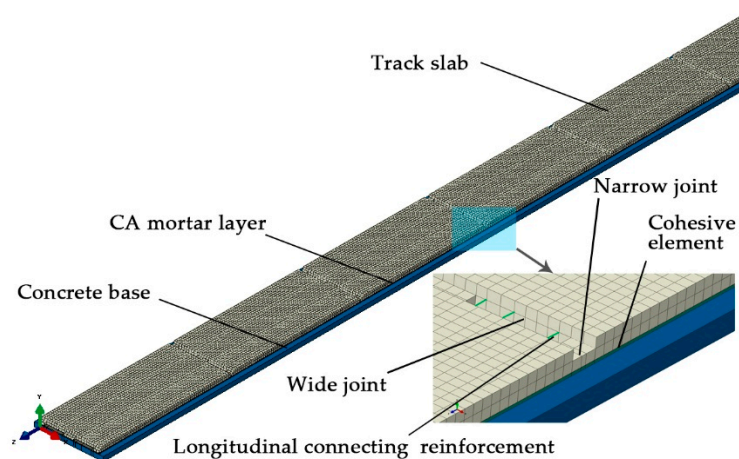
161 The damage value D , proposed by Camanho and Davila [19], is defined as:

$$D = \frac{\delta_m^f (\delta_m^{\max} - \delta_m^0)}{\delta_m^{\max} (\delta_m^f - \delta_m^0)} \quad (2)$$

162
 163 Where δ_m^0 is the effective displacement of the element node when the failure starts. δ_m^f is the
 164 effective displacement of the node when the damage value D reaches 1. δ_m^{\max} is the maximum
 165 displacement of nodes in the load history. $0 < D < 1$ means that the interface element is in the softening
 166 area, and when the D value is 1, it means that the interface element is broken.

167 3.2 Finite element model and model parameters

168 In order to study the influence of tension value on the track slab and interface between track
 169 slab and CA mortar, a three dimensional finite element model of CRTSII slab ballastless track is built
 170 according to the actual size of ballastless track based on the commercial software ABAQUS, as
 171 shown in Figure 6. The track slab, mortar layer and concrete base are all simulated by solid elements,
 172 and the longitudinal reinforcement which is constrained by the joint with the track slab concrete is
 173 simulated by truss element. The cohesive element described in the above section is disposed on the
 174 bonding layer between the concrete of the track slab and the mortar layer, the debonding of interface
 175 is simulated by the failure of bonding layer element. Tie constraints are applied between the mortar
 176 layer and the concrete base and all the displacements of the nodes at the bottom of the slab track
 177 system are restricted. The model has a total length of 39 m (six track slab) and the parameters are
 178 shown in Table 1.



179
 180 **Figure 6.** Finite element model

182

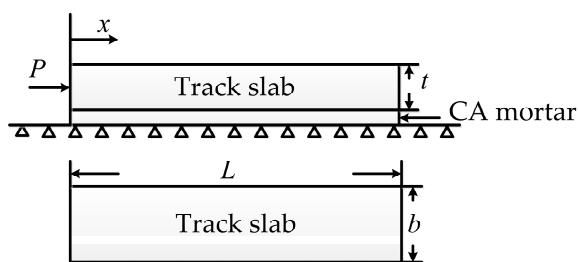
Table 1. Parameters of slab ballastless track model

Components	Young's modulus (Pa)	Poisson ratio	Thermal expansion coefficient ($^{\circ}\text{C}^{-1}$)
Track slab	3.25E+10	0.2	1E-5
CA mortar	8E+9	0.2	-
Concrete base	2.55E+10	0.2	-

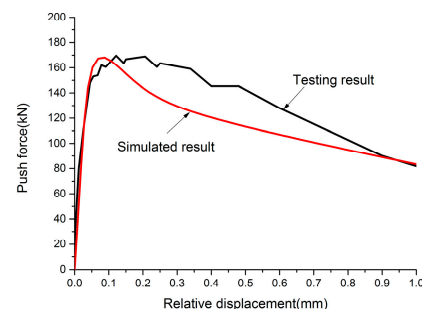
183 Load-displacement curve of the interface is obtained by slab push test on single rail pads
 184 carried out by China Academy of Railway Sciences Corporation Limited (CARS). In order to get the
 185 parameters of the interface element, a three-dimensional finite element model is established
 186 according to the actual size and constraint mode of the single rail pads push slab test (shown in
 187 Figure 7a). $L=2.55\text{m}$, $b=0.65\text{m}$, $t=0.2\text{m}$. Loading method is simulated by gradually increasing the
 188 displacement of the track slab end.

189 This paper assumes that the normal stress strength is the same as the shear stress strength, for
 190 the reason that the normal stress value is much smaller than the shear stress value in the process of
 191 pushing test and the normal stress strength is slightly greater than the shear strength based on the
 192 interface experiment [20], which result in a conservative result.

193 Figure 7b shows the simulation results, the simulated load-displacement curve is most
 194 consistent with the experimental results with $\tau_f=0.075\text{MPa}$, $\delta_1=0.1\text{mm}$, $\delta_f=2\text{mm}$. It can be seen that
 195 the established model agrees well with the experimental results in the ascending phase, while the
 196 push force is slightly smaller than the test results in the descending phase. But overall, there is a
 197 good consistency for the fitting result, which proves that cohesive parameters are reasonable and
 198 credible.



(a) Push test on single rail pad



(b) Testing and simulated result of push test

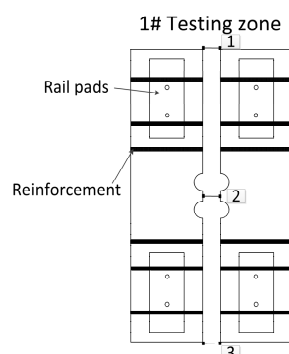
199

Figure 7. Push test on single rail pad and its result

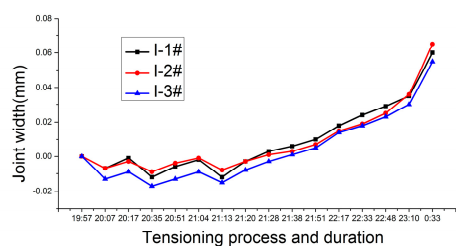
200 3.3 Experimental verification

201 Tensile test is carried out on the end joint of rail plate by the CARS [20]. The measuring point
 202 location and measurement results are shown in Figure 8.

203



(a) Measuring point of tensioning of longitudinal connecting reinforcement



(b) Testing result of tensioning of longitudinal connecting reinforcement

204

Figure 8. Tension points and test results of longitudinal reinforcement

205 The tension of reinforcement in the measured track can cause the joint compression at the end
206 of the plate (the point of break in the figure). The total compression amount of the joint for 1# and 2#
207 measurement area after tension of reinforcement is -0.026mm and -0.020mm respectively. The
208 shrinkage of track structure after reinforcement tensed in the condition of temperature reduction
209 causes the joint of slab end expand obviously. The maximum extension of track slab joint is closed to
210 0.08 mm when the temperature drop 5°C in the actual measurement period from 21:00 to 1:00(the
211 end of Figure 8(b) curve).

212 The longitudinal connected reinforcement at the slab end is tensioned in the tensile order. The
213 calculated tensile displacement of the three measuring points are 0.021mm, 0.028mm and 0.021mm
214 respectively for the simulation model, which is very close to the measurement result. In addition,
215 the track slab is applied -5°C cooling load after longitudinal connected reinforcement tensioned, the
216 opening displacement at the end of the track slab was 0.07mm, which was close to the measured
217 results, and proved the reliability of the model.

218 4. Mechanical analysis in tensioning process

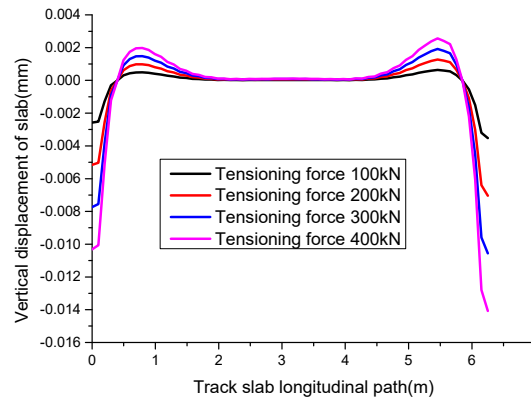
219 Each longitudinal connecting reinforcement provides 50kN tension force when the longitudinal
220 connecting reinforcement of ballastless track is stretched. Tension force is simulated by dropping
221 temperature, the equivalent formula is:

$$222 \Delta t = \frac{\Delta l}{l\alpha} = \frac{F}{AE\alpha} \quad (3)$$

223 Where Δt is the scale of drop in temperature, Δl is the length change of wide joint, l is the length
224 of wide joint, α is coefficient of linear expansion, F is the tension value, A is the section area of
225 longitudinal connecting reinforcement, E is the elastic modulus of longitudinal connecting
226 reinforcement.

227 The ballastless track will be affected by the temperature load after the longitudinal
228 reinforcement is stretched and before the casting of the wide joint, only the temperature gradient
229 load caused by daily temperature change is considered due to the short time interval between
230 casting and stretching. Taking common temperature gradient load into consideration, positive
231 temperature gradient load is 50°C / m and negative temperature gradient load is -25°C / m,
232 temperature gradient loads are applied after the longitudinal reinforcement is tensioned. The
233 designed tension load is 300kN, so here four calculation conditions of 100kN, 200kN, 300kN and
234 400kN are selected to analyze the influence of tension load.

235 The vertical displacement of the bottom side of the track slab after longitudinal connected
236 reinforcement tensioned is shown in Figure 9. It can be seen that due to the existence of narrow joint,
237 the longitudinal connecting reinforcement makes the track slab under eccentric compression after
238 stretching. The narrow joint position is under compression, the track slab tends to arch upward. The
239 arch displacement of the track slab is increasing from the position of the slab edge to the position
240 0.7m away from the slab edge. The arch displacement of the track slab begins to decrease gradually
241 and then tends to be very small from the position of 0.7m away from the slab edge to the position of
242 2m away from the slab edge. The larger the tensile force is, the larger the arch displacement is, and
243 the relationship between the arch displacement and tensile force is nearly liner relationship. The
244 arch displacement of the track slab is very small (0.002mm) for ballastless track structure.



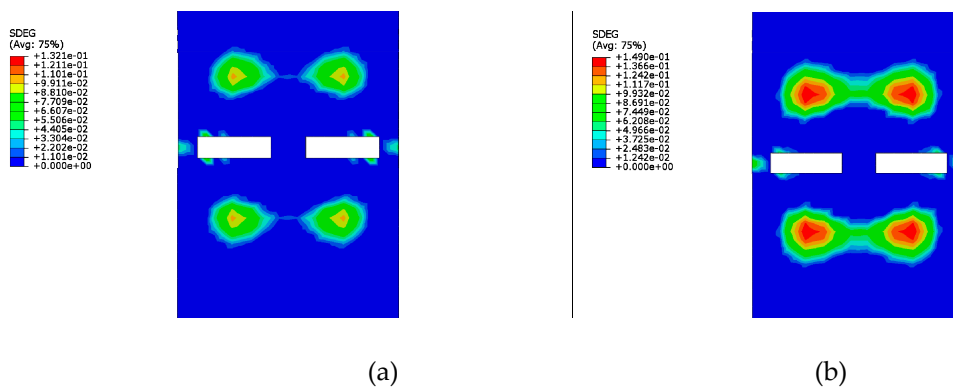
245
246
247

Figure 9. Vertical displacement of track slab after longitudinal connecting reinforcement is tensioned

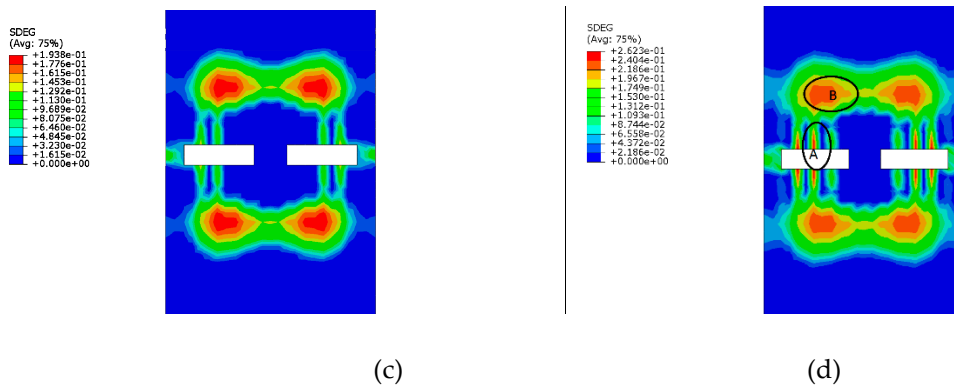
248 Figure 10. shows the damage at interface between track slab and CA mortar under the action of
249 positive temperature gradient load with different tensile force values. It can be seen that the position
250 of the interface damage is located 0.7m away from the edge of the track slab and edge of the track
251 slab that corresponds to the outer reinforcement under the action of positive temperature gradient
252 load. Both the damage value and the damage area increase with the increase of the tension force
253 value. The position where the damage first appears is 0.7m away from the edge of the track slab
254 (point B) and the temperature gradient load value when the interface damage occurs is reduced from
255 $46^{\circ}\text{C}/\text{m}$ to $40^{\circ}\text{C}/\text{m}$ when the tension force value increases from 100kN to 300kN (shown in Figure 11).
256 But when the tension force value is 400kN, the first damage area at the edge of the track slab (point
257 A) and the corresponding temperature gradient load value is $20^{\circ}\text{C}/\text{m}$, which explains that the large
258 tension force value is unfavorable to the interface at the end of the track slab.

259 The stress condition of the element node at point A and point B are shown in Figure 12 and
260 Figure 13. It is longitudinal shear stress rather than the vertical normal stress and transverse shear
261 stress that is most affected by tension force value. The three-direction stress of the interface element
262 increases linearly with the increase of positive temperature gradient load. The failure mode at point
263 B is mixed failure for its three-direction stress are relatively large. Point A is subjected to 62200Pa of
264 longitudinal shear stress when the tension process ends. When the positive temperature gradient
265 load reach $20^{\circ}\text{C}/\text{m}$, Point A begins to appear damage under longitudinal shear stress and transverse
266 shear stress, so the failure mode at point A is shear failure.

267

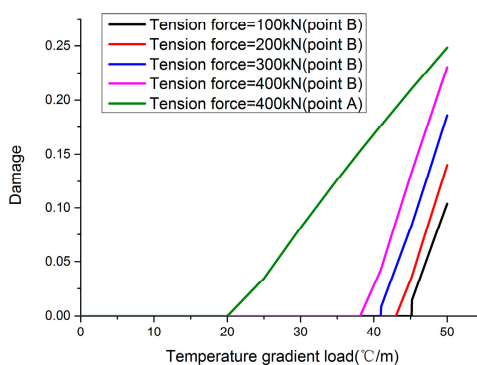


268
269
270



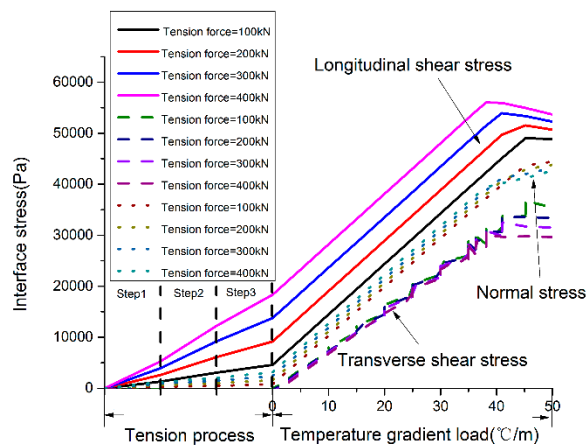
271
272
273
274
275

Figure 10. Damage evolution under positive temperature gradient load with different tension force (a)-(d), 100kN - 400kN.



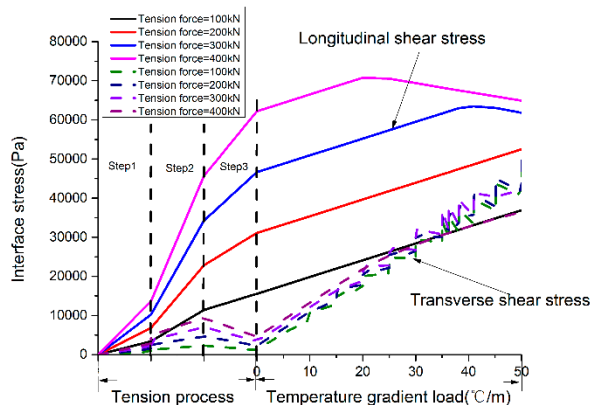
276
277
278

Figure 11. Damage evolution at point A and point B



279
280

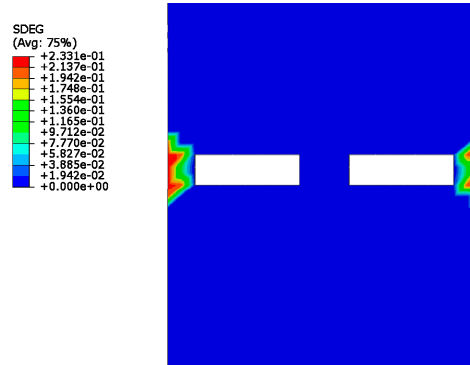
Figure 12. Interface stress evolution at point B



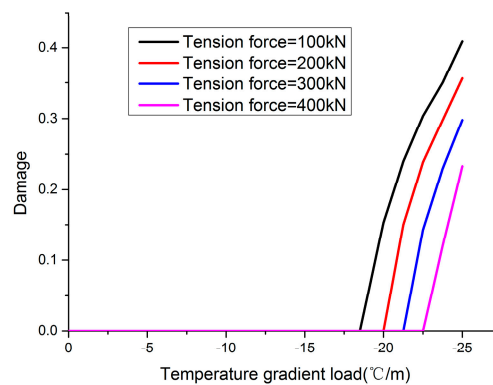
281
282

Figure 13. Interface stress evolution at point A

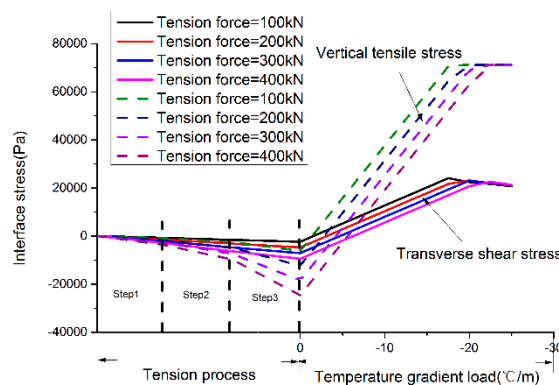
283 The interface damage areas shown in Figure 14 are located at the narrow joint position under
 284 the action of negative temperature gradient load with different tension force values. The damage
 285 value reduced from 0.453 to 0.233 and temperature gradient load value when the interface damage
 286 occurs is reduced from $-22.5^{\circ}\text{C}/\text{m}$ to $-18.5^{\circ}\text{C}/\text{m}$ when the tension force value increases from 100kN to
 287 400kN(as shown in Figure 15). The stresses of the interface in the damaged area are shown in Figure
 288 16. Narrow joint position damage is mainly caused by vertical normal stress. The greater the tension
 289 force value is, the greater the buckle pressure to the narrow joint position. So the longitudinal
 290 tension of reinforcement can reduce the warping of the track slab corner.
 291



292 **Figure 14.** Damage evolution under negative temperature gradient load with 400kN tensile
 293 forces
 294



295 **Figure 15.** Damage evolution under negative temperature gradient load
 296
 297



298 **Figure 16.** Interface stress evolution at point A
 299

300 The tension force of the longitudinal reinforcement has little effect on the deformation and
 301 stress of the track slab, however, interface damage occurs between the track slab and the mortar
 302 layer when subjected to temperature gradient load after the end of tension process. For interface
 303 damage, the tension force of the longitudinal reinforcement increases the interface shear stress at the

304 edge of the track slab and produces a downward depressing pressure which is possible to increase
 305 the ability to resist negative temperature loads, but to reduce the ability to resist positive
 306 temperature gradient loads. Therefore, the casting of the wide joint should be carried out at the same
 307 time or as soon as possible after the longitudinal reinforcement is stretched to avoid a damage
 308 between the layers under large temperature gradient load and ensure a reliable connection between
 309 the mortar layer and the track slab.

310 4. Check and calculation in operating period

311 4.1 Original design check and calculation

312 300kN prepressure is applied to the concrete at the wide and narrow joint by applying 300kN
 313 longitudinal tension force to the longitudinal reinforcement between the track slabs in the design,
 314 and the track slab is considered as continuous in the longitudinal direction. The track slab is
 315 considered as the bar fixed in beam end. Therefore, the strain of the track slab under the action of
 316 system temperature difference is:

$$317 \quad \varepsilon_{\Delta T} = \alpha \Delta T \quad (4)$$

318 The shrinkage deformation considered from 14 days to infinity of concrete is carried out
 319 according to the specification [8]. The contraction strain is:

$$320 \quad \varepsilon_s = -0.23 \quad (5)$$

321 The stress of the reinforcement under the action of live load is not taken into account but only
 322 cooling and concrete shrinkage load are considered in the calculation for the reason that the
 323 longitudinal connecting reinforcement of the track slab is placed in the middle of the track slab. The
 324 stress of reinforcement is:

$$325 \quad \sigma_s = E_s \cdot (\varepsilon_{\Delta T} + \varepsilon_s) \quad (6)$$

326 Where E_s is elastic modulus of reinforcement.

327 There are only six $\Phi 20$ connecting reinforcement in the joint of the track slabs. The stress of the
 328 reinforcement at the joint and the crack width is checked and calculated according to the tensile
 329 check result of the reinforcement inside the track slab. The axial force borne by the track slab is as
 330 formula (7) under the combined action of cooling load and shrinkage load.

$$331 \quad N = \sigma_s \cdot A_s \quad (7)$$

332 Where A_s is cross-sectional area of a single connecting reinforcement.

333 The stress of reinforcement caused by shrinkage and cooling of concrete in the future should be
 334 superimposed on the stress caused by tension of connecting reinforcement for the reason that the
 335 tension step occurred before concrete casting step. In addition, the pre-stress of the joint cannot play
 336 a role in limiting the crack width due to the fact that the joint concrete is not perfused when the
 337 tension force is applied to the connecting reinforcement.

338 The stress of connecting reinforcement at the wide joint is:

$$339 \quad \sigma_{s,c} = (N + N_{ten}) / A_{s,all} \quad (8)$$

340 Where $A_{s,all}$ is total cross-sectional area of six reinforcement. N_{ten} is tension force.

341 The average strain of reinforcement is:

$$342 \quad \varepsilon_{s,a} = N / E_s / A_{s,all} \quad (9)$$

343 Crack width is checked and calculated according to the formula below:

$$344 \quad \omega_{cr} = l_{cr,max} \cdot (\varepsilon_{s,a} - \varepsilon_{c,a}) \quad (10)$$

345 Where ω_{cr} is calculated value of crack width, mm. $l_{cr,max}$ is maximum crack spacing, mm. $\varepsilon_{s,a}$ is
 346 average strain of reinforcement. $\varepsilon_{c,a}$ is average strain of concrete.

347 Take the distance (650mm) between the false seam of track slab as $l_{cr,max}$. As the strain of
 348 concrete is much smaller than that of reinforcement, the average strain of concrete is considered to
 349 be 0.

350 The limiting design value of reinforcement stress is 286MPa and the crack width is 0.5mm
 351 according to the design specification [8]. The reinforcement stress is 577.6MPa and crack width is
 352 0.65mm calculated by equations (8) and (10) and both the calculation results are not meet the design
 353 requirements.

354 It can be seen from formula (8) that the stress value of connecting reinforcement can be reduced
 355 by reducing tensile force of connecting reinforcement. In order to reduce the crack width, the
 356 effective measures are to reduce the diameter of connecting reinforcement or to apply pre-stress to
 357 the wide joint concrete.

358 4.2 Application of pre-stressed on post-cast concrete

359 Temperature pre-stress loss can be occurred in steam curing causes for pretensioning
 360 pre-stressed concrete for the reason that expansion of pre-stressed reinforcement with higher
 361 temperature. When the concrete compressive strength reaches a certain strength grade, as 7.5MPa to
 362 10MPa, the reinforcement and concrete are considered as a whole, which can expand and contract
 363 together without causing stress loss. But for the wide joint concrete of ballastless track, here we have
 364 a design mistake. The pre-stressed reinforcement is not loose after the casting of wide joint concrete
 365 which is different with pretensioning pre-stressed concrete, so it is not possible to generate pre-stress
 366 on the wide joint concrete.

367 Here we propose a method of applying pre-stress to the post-pouring concrete between the old
 368 concrete reference the concept of pre-stress loss for pretensioning pre-stressed concrete.

369 After the concrete is casting, electrode heating is applied to connecting reinforcement, which
 370 makes the temperature increase for connecting reinforcement. To makes the temperature difference
 371 between the pre-tensioned reinforcement and the cast concrete, we can apply thermal insulation
 372 material on the surface of the reinforcement. The pre-tensioned reinforcement relaxes to make the
 373 tension force decreases. When the concrete compressive strength reaches 7.5MPa to 10MPa, the
 374 concrete and tensile reinforcement will deform together. When the concrete and reinforcement
 375 resume to its initial temperature, a part of tensile force of the reinforcement will be lost and a part of
 376 pre-stress will be generated to the post-pouring concrete which the pre-stress value is equal to the
 377 lost tensile force of reinforcement.

378 4.3 Calculation of reasonable tension value

379 The pretension loss value is determined by the temperature difference between concrete and
 380 reinforcement when the concrete and reinforcement deforms together. The pretension decreases as
 381 formula (11) when the temperature difference is Δt .

382 When the reinforced concrete deforms together:

$$383 N_{los} = \Delta t \alpha E_s A_{s,all} \quad (11)$$

384 Pre-stress of concrete $N_{pre} = N_{los}$.

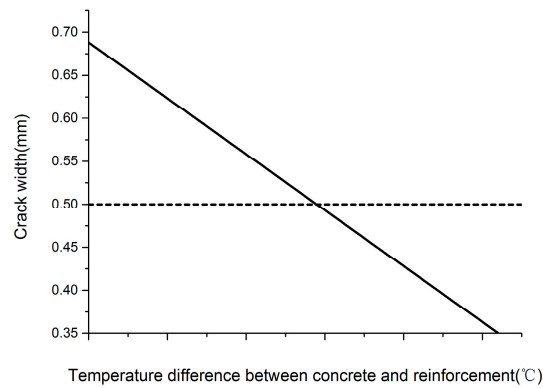
385 At this time the stress of connecting reinforcement is:

$$386 \sigma_{s,c} = (N + N_{ten} - N_{los}) / A_{s,all} \quad (12)$$

387 The strain of connecting reinforcement is:

$$388 \varepsilon_{s,a} = (N - N_{pre}) / E_s A_{s,all} \quad (13)$$

389 From equations (10), (11) and (13), it can be seen that the crack width is only related to the value
 390 of the pre-stress generated at the wide joint, while the pre-stress value is related to the temperature
 391 difference Δt inside reinforced concrete. Figure 17 shows the relationship between the crack width
 392 and temperature difference value between concrete and reinforcement. It can be seen that
 393 reinforcement and concrete temperature difference value should not be less than 29 °C to guarantee
 394 the crack width is less than 0.5 mm.



395
396
397

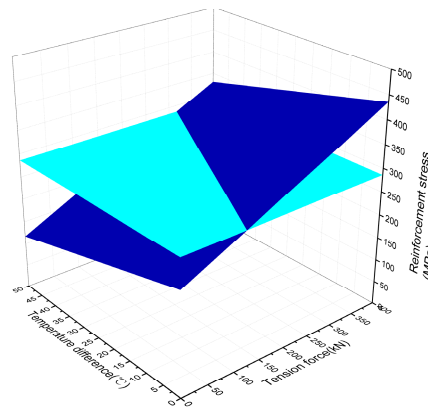
Figure 17. The relationship between crack width and temperature difference between concrete and reinforcement

398
399
400
401
402
403
404
405
406

It can be seen from formula (10) and (12) that the stress of reinforcement is related to tension force and internal temperature difference between concrete and reinforcement. Figure. 18 shows the three-dimensional diagram of stress, tension of reinforcement and temperature difference. It can be seen that stress of reinforcement is directly proportional to tension force and inversely proportional to temperature difference. According to the checked results of crack width, the temperature difference value should be greater than 29 °C, the three-dimensional figure is mapped to the tension in the Figure 18 - flat surface temperature difference value, under the condition of guaranteeing the crack width and the reinforcement stress meet the design requirements of tension and temperature range, as shown in Figure 19 shaded area.

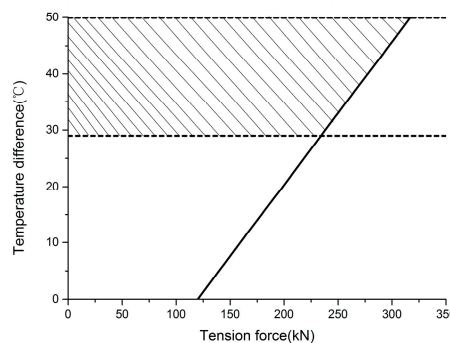
407
408
409
410

The maximum tensile force should not exceed 234kN under the condition that the crack width meets the design requirements, maximum tension force linearly increases with the rising of the reinforced concrete temperature difference. The maximum tension force should not exceed 317 kN when reinforced concrete temperature difference value is 50 °C.



411
412
413

Figure 18. The relationship among reinforcement stress and tension force and temperature difference value



414

415 **Figure 19.** Temperature and tension force range to guarantee appropriate reinforced stress and
 416 crack width

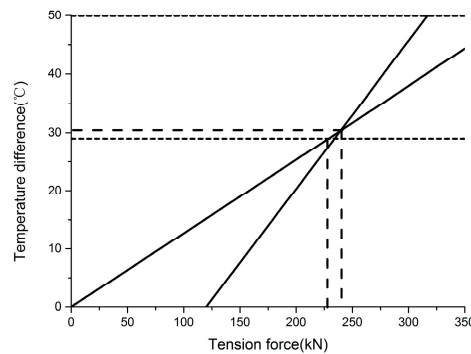
417 Before the casting of wide-seam concrete, the track slab is in an eccentric compression state after
 418 the longitudinal reinforcing bar is stretched due to the existence of narrow joint.

419 In order to ensure the track slab has a symmetry stress station after the casting of wide-seam
 420 concrete, the temperature increment value of the precast reinforcement should be determined
 421 according to different tensile values.

422 The tensile force at this point is

$$423 N_{ten} = 2N_{los} = 2\Delta t\alpha E_s A_{s,all} \quad (14)$$

424 Figure 20 shows the relation between tensile force value and temperature increment value of
 425 reinforcement under the condition of ensuring that the stress of reinforcement and crack width of
 426 concrete meet the requirements and at the same time ensuring the tension force value of track slab
 427 under the symmetry pressure condition. It can be seen that tension force range is 229 kN to 240 kN
 428 and temperature difference range is 29°C to 30.3°C to meet the design requirements and tensile
 429 force does not cause interface failure between the track slab and the mortar layer. Due to the range of
 430 tension force value and temperature difference of reinforcement is relatively small, so it is suggested
 431 that selection of tension force value is 230 kN and temperature difference of reinforcement is 30°C
 432 during construction.



433 **Figure 20.** Reasonable tension value and temperature difference value range
 434

435 5. Conclusions

436 In this paper, a cohesive zone model is introduced in a three-dimensional finite element model
 437 of CRTSII slab track and utilized to investigate the damage or delamination at the interface between
 438 track slab and CA mortar layer during the construction stage. The interface stress and damage
 439 evolution under the condition of different tension force value and temperature gradient load are
 440 analyzed. Simulation results show that interface damage is occurred under temperature gradient
 441 load at the end of track slab for large longitudinal shear stress is produced when the tension force is
 442 greater than 300kN. A method of applying pre-stress to post-pouring concrete is proposed according
 443 to the concept of pre-stress loss of pretensioning pre-stressed concrete, crack width and the
 444 reinforcement stress of the ballastless track in the operation stage were checked and calculated
 445 according to the concrete design principle. The tension value is suggested in 230 kN, meanwhile, be
 446 sure temperature difference between reinforcement and concrete value is 30°C before initial curdle
 447 of concrete.

448 Future developments of present work will focus on experimental verification activities in terms
 449 of applying prestressing on post concrete. A simple construction method is also needed for
 450 operating line and conduct on-site experiments and evaluation of this method.

451 **Author Contributions:** Long Chen carried out the research work together with Jian-xi Wang, Jin-jie Chen is the
 452 head of the chair of Traffic Engineering and provides general support to all the activities of the research staff
 453 and provide data support for this research.

454 **Funding:** This research was funded by Natural Science Foundation of Hebei Province under grant E2016210131
455 and Key Project of Science and Technology Research of High Education in Hebei Province under grant
456 ZD2015037.

457 **Conflicts of Interest:** The authors declare no conflict of interest.

458

459 References

- 460 1. Esveld, C. Recent developments in slab track, *Eur. Railway Rev.* 9 (2003) 81 – 86.
- 461 2. Esveld, C. Developments in high-speed track design, keynote lecture at: structures for high-speed railway,
462 in: Transportation-IABSE Symposium, Antwerp, 2003. pp. 27– 29.
- 463 3. He, H.-W. *Ballastless Track Technology*; China Railway Press: Beijing, China 2005.
- 464 4. Li, D.-S. Performance of CRTS II Slab Ballastless Track on the High Speed Railway Bridge. Ph.D. Thesis.
465 China Academy of Railway Sciences, Beijing, China 2016.
- 466 5. Li, P.-G. Analysis of the Interface Damage of CRTS II Slab Track and Its Influences. Ph.D. Thesis.
467 Southwest Jiaotong University, Chengdu, China 2015.
- 468 6. Liu, Z.; Ding, C.-X.; Hu, J.; et al. Tension Force Analysis of CRTS II Slab type Ballastless Track Caused by
469 Widening Joint Between Track Slabs. *Railway Engineering*, 2016, 5:69-72.
- 470 7. Gao, L.; Liu, Y.-A.; Zhong, Y.-L.; et al. Influence of Damage of Wide and Narrow Joints on Mechanical
471 Performance of CRTS II Slab type Ballastless Track CWR. *Railway Engineering*, 2016, 5:58-63.
- 472 8. Deutsches Institut Fur Normung. DIN 1045-1-2001, Concrete, reinforced and prestressed concrete
473 structures - Part 1: Design and construction [S]. Berlin: Deutsches Institut Fur Normung, 2001.
- 474 9. Dugdale, D. Yielding of steel sheets containing slits, *J. Mech. Phys. Solids* 8(1960) 100 – 104.
- 475 10. Barenblatt, G. The formation of equilibrium cracks during brittle fracture: general ideas and hypothesis,
476 axially symmetric cracks, *Appl. Math. Mech. (PMM)* 23 (1959) 622 – 636.
- 477 11. Barenblatt, G. Mathematical theory of equilibrium cracks in brittle fracture, *Adv. Appl. Mech.* 7 (1962) 55–
478 125.
- 479 12. Alfano, G.; Crisfield, M.-A. Finite element interface models for the delamination analysis of laminated
480 composites: mechanical and computational issues, *Int. J. Numer. Methods Eng.* 50 (2001) 1701– 1736.
- 481 13. Chen, J.; Crisfield, M.; Kinloch, A.; Busso, E.; Matthews, F.; Qiu, Y. Predicting progressive delamination of
482 composite material specimens via interface elements, *Mech. Compos. Mater. Struct.* 6 (1999) 301– 317.
- 483 14. Petrossian, Z.; Wisnom, M. Prediction of delamination initiation and growth from discontinuous plies
484 using interface elements, *Compos. Part a – Appl. Sci. Manuf.* 29 (1998) 503– 515.
- 485 15. Camanho, P.; Davila, C.; Moura, M. Numerical simulation of mixed-mode progressive delamination
486 in composite materials, *J. Compos. Mater.* 37 (2003) 1415–1438.
- 487 16. Borg, R.; Nilsson, L.; Simonsson, K. Simulating DCB, ENF and MMB experiments using shell elements and
488 a cohesive zone model, *Compos. Sci. Technol.* 64 (2004) 269– 278.
- 489 17. Jiang, W.; Hallett, S.; Green, B.; Wisnom, M. A concise interface constitutive law for analysis of
490 delamination and splitting in composite materials and its application to scaled notched tensile specimens,
491 *Int. J. Numer. Methods Eng.* 69 (2007) 1982– 1995.
- 492 18. Chen, L.; Chen J.-J.; Wang, J.-X. Study On Stress Transfer and Interface Damage of CRTSII slab ballastless
493 track, *J Chin Railway Soc.* 2018,40(08):130-138.
- 494 19. Camanho, P.P.; Davila, C.G.; *Mixed-Mode Decohesion Finite Elements for the Simulation of Delamination*
495 *in Composite Materials*, NASA/TM-2002-211737, 2002, pp. 1– 37.
- 496 20. Zhao L. Spatial Refinement Analysis Method of High Speed Railway Ballastless Track and Its Application
497 Research. Ph.D. Thesis. Beijing Jiaotong University, Beijing, China 2015.